JOURNAL OF MATERIALS SCIENCE 35 (2000) 2507–2515

Yield behavior and failure response of an aliphatic polyketone terpolymer subjected to multi-axial stress states

N. R. KARTTUNEN, A. J. LESSER*
Polymer Science and Engineering Department, University of Massachusetts, Amherst, Massachusetts 01003, USA

The yield behavior of an engineering thermoplastic under biaxial stress states has been investigated. The material considered is an aliphatic polyketone terpolymer. Multiaxial testing was performed on thin-walled hollow cylinders at four different temperatures and three strain rates. Various stress states were applied in order to develop failure envelopes. Within each envelope, the nominal strain rate along the octahedral shear plane, $\dot{\gamma}^{oct}$, was held constant. These tests were performed at 0, 20, 50 and 80°C at $\dot{\gamma}^{oct} = 0.05$ min^{-1}. At 20°C, samples were also tested at $\dot{\gamma}^{oct} = 0.005$ and 0.5 min^{-1}. Below the T_g of 12°C, failures in all stress states investigated, except axial compression, were brittle. At temperatures of 50 and 80°C, all failures were ductile. At 20°C, both ductile and brittle failures were observed. Although the rate affected the yield strength of the material, it had little effect on the mode of failure. In contrast, the temperature had a significant effect on the yield strength and mode of failure. While the effect of strain rate on yield strength was greater in the hoop direction than axial, the opposite was true for the effect of temperature. It was also observed that the state of stress played a significant role in the material failure.

1. Introduction

The use of polymers in engineering applications has made the mechanical characterization of these materials essential. It is also important to consider the effects of strain rate and temperature since they have significant influence on the yield behavior. The uniaxial tensile behavior of many polymers has been well characterized. However, as many applications involve multiaxial stress states, it is especially important to investigate material behavior under these conditions as well. Unfortunately, relatively few studies to date have looked into this subject matter.

Many of the studies that have investigated the yield behavior of polymers subjected to multiaxial stress states have focused on glassy polymers. Bowden and Jukes [1] studied sheets of amorphous polymethylmethacrylate in plane strain compression with tension applied normal to the compression direction. Another investigation was done by Carapellucci and Yee [2] on the yielding of slightly anisotropic polycarbonate cylinders. Specimens were loaded axially and silicone oil was used to pressurize the cylinders internally. The study did not include the effect of test rate, but did consider two different test temperatures and different degrees of anisotropy. More recently, Kody and Lesser [3, 4] studied isotropic epoxy systems, elucidating the effects of strain rate, temperature, as well as molecular architecture on the yield and fracture behavior. In their work, hollow cylinders were loaded axially in either tension or compression and nitrogen gas was used for pressurization.

Some thermoplastic materials have also been investigated. Mittal and Singh [5] studied the deformation behavior of nylon-6 and amorphous PMMA under uniaxial and biaxial loading. The samples were cut and machined from commercially available tubes and were tested in tension, torsion, and combined tension and torsion loadings.

Tuttle, Semeliss and Wong [6] studied the elastic and yield behavior of slightly anisotropic polyethylene. Extruded tubes were tested at room temperature under a constant octahedral shear stress rate of 1.78 MPa/min along all loading paths. Yield was defined as the 0.3% offset in the octahedral shear stress versus octahedral shear strain curve. Effects of temperature, test rate and degree of orientation were not considered.

Bekhet, Barton and Craggs [7] studied the yield behavior of highly oriented polypropylene tubes in which different degrees of orientation were produced by die drawing prior to testing. Testing was performed under maximum principal strain rate control at room temperature. Strain rates were between 120–200 s^{-1}. The yield point was defined in the study as the 0.5% offset in the equivalent stress versus equivalent strain curve.

* Author to whom all correspondence should be addressed.

While different levels of orientation were included in the study, effects of temperature or test rate were not considered.

Some of the previous studies have been conducted on either isotropic or highly oriented specimens. Because processing techniques such as extrusion, injection molding, etc., typically induce a small degree of orientation, it is appropriate to study mildly anisotropic materials. The present investigation is performed on extruded pipe, as received from the resin supplier. The testing geometry allows a wide range of stress states to be applied to the specimens by controlling the ratio between the axial load and internal pressure. Moreover, by maintaining a constant $\dot{\gamma}^{oct}$ for all stress states within a failure envelope, the rate effects between envelopes can be compared. The effects of temperature on the yield behavior have also been studied. The yield point will be defined here as the point at which a zero slope condition is achieved in the octahedral shear stress/volumetric strain curve.

2. Experimental

2.1. Material and specimen preparation

The polymer tested in this investigation is a semicrystalline aliphatic polyketone. This engineering thermoplastic has recently been introduced by Shell Chemical Company under the trademark Carilon®. The structure of the polymer consists of perfectly alternating units of carbon monoxide and ethylene, with a small proportion of the ethylene units substituted with propylene units (approximately 6 mol %). The glass transition temperature, T_g, of the terpolymer is approximately 12°C. Mechanical properties of Carilon® have been shown to be competitive with those of nylon 6,6, polyacetals, and other engineering thermoplastics [8–11].

Uniaxial and biaxial tests were conducted on thin walled hollow cylinders. The specimen gripping system is shown in Fig. 1. Cylindrical specimens were cut at 150 mm lengths from extruded pipe with an external diameter of 22.3 mm and a wall thickness of 1.95 mm. This length was sufficient to neglect end effects in the center region of the cylinders. For each specimen, steel inserts were placed into the ends of a hollow cylinder, and compression fittings placed around the cylinder. The fitting "sealed" the specimen for pressurization. At each end the specimen was secured to a pipe fitting, which was then threaded into steel cylinders. The steel cylinders were clamped into grips attached to a tension-torsion machine, described in the next section. The upper steel cylinder was tapped to allow internal pressurization of the specimens. Nylon cord was inserted into the hollow cylinders to reduce the compressible volume.

2.2. Experimental procedure

Hollow cylindrical specimens were subjected to uniaxial and biaxial states of stress at either 0, 20, 50 or 80°C at an octahedral shear strain rate, $\dot{\gamma}^{oct}$, of 0.05 min^{-1}. In addition, at 20°C, samples were also tested at $\dot{\gamma}^{oct} =$ 0.005 and 0.5 min^{-1}. Specimens were conditioned for 30 minutes at the appropriate temperature prior to testing, except for the 0°C tests where a 60 minute conditioning time was used. Tests were performed in an Instron 1321 tension-torsion machine modified with a Tescom ER3000 pressure regulator, Fig. 2. Both were controlled externally with a personal computer. For each test, the specific stress state was regulated by the test program as the specimen was loaded to failure. Nitrogen gas was used to pressurize the cylinders. Each of the stress states within a given failure envelope was applied at the same octahedral shear strain rate. This was chosen as the method of control because the octahedral shear stress, τ^{oct}, is utilized in several failure theories typically based on Von Mises' theory. Modifications of Von Mises' theory have been shown to fit the behavior of polymeric materials fairly well [3, 12].

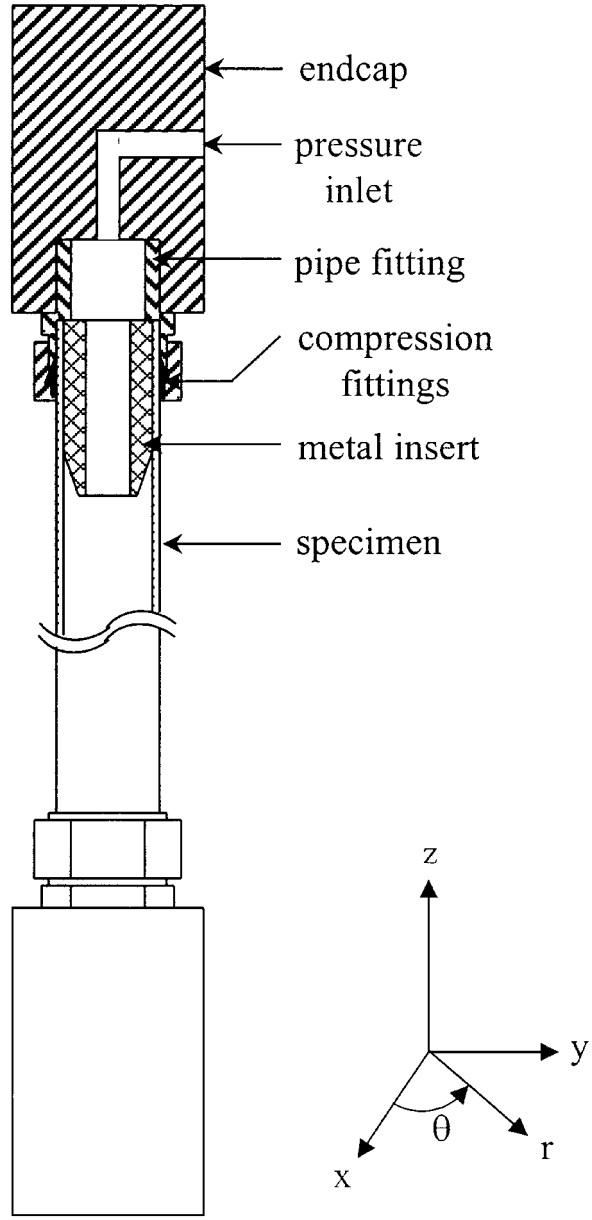

Figure 1 Endcap fixture for hollow cylinder testing. Coordinate system is indicated.

All tests in this study were conducted in a pseudo-strain controlled mode whereby the nominal octahedral shear strain was maintained at a constant rate. The octahedral shear strain was calculated from the applied stresses using a constitutive relationship appropriate for transversely isotropic linear-elastic viscoelastic materials (see Appendix). The material properties needed for

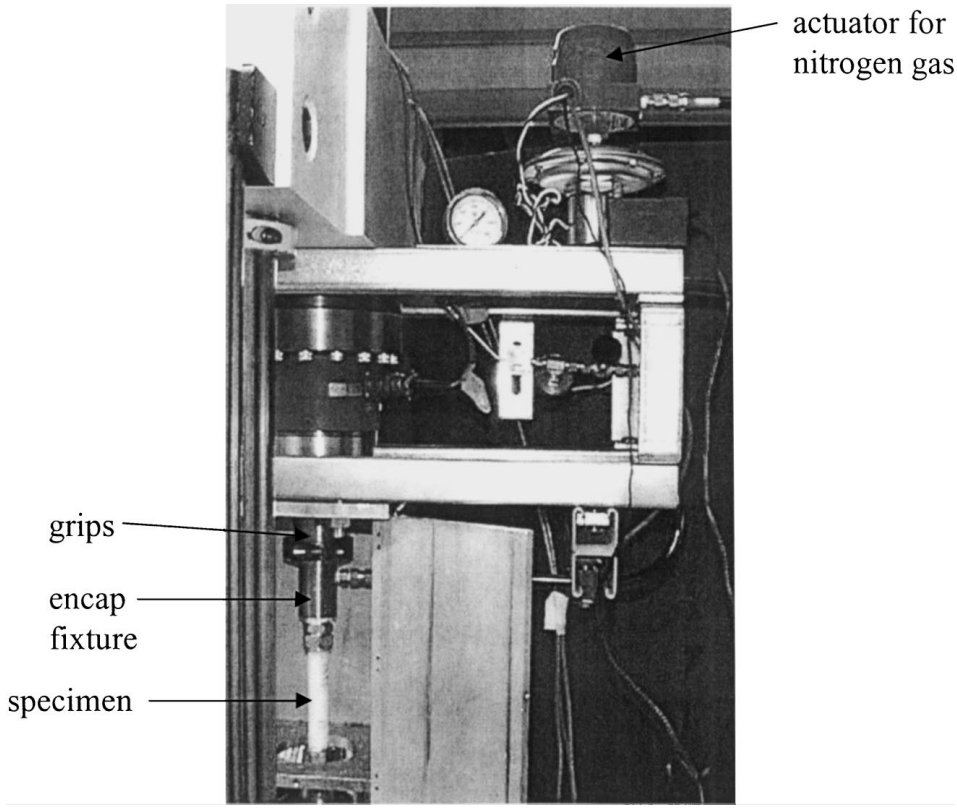

Figure 2 Biaxial testing apparatus for hollow cylinder specimens. Axial tension or compression may be applied with simultaneous internal pressurization.

this calculation were obtained by conducting tests in four different stress states on hollow cylinders with two extensometers attached to each cylinder. The tests were conducted by applying different proportional loading conditions for each test and measurements of the axial and hoop strains were recorded. Note that these specimens were not taken to failure to avoid damage to the extensometers. The radial strain was assumed to equal the hoop strain in these calculations and was not measured directly (i.e., considerations based on a transversely isotropic morphology). This data was then used to calculate the material coefficients for a transversely isotropic material loaded in its principal directions (see Appendix).

The coefficients together with the constitutive relationship (see Appendix) were then used in subsequent tests to continually calculate the nominal octahedral shear strain and appropriate loading rate in order to keep the nominal octahedral shear strain rate constant. The nominal octahedral shear strain rate, $\dot{\gamma}^{\text{oct}}$, was calculated from Equation 1:

$$\dot{\gamma}^{\text{oct}} = \frac{1}{3}\sqrt{(\dot{\varepsilon}_\text{r} - \dot{\varepsilon}_\text{z})^2 + (\dot{\varepsilon}_\text{z} - \dot{\varepsilon}_\theta)^2 + (\dot{\varepsilon}_\theta - \dot{\varepsilon}_\text{r})^2} \quad (1)$$

where $\dot{\varepsilon}_\text{z}$, $\dot{\varepsilon}_\text{r}$, and $\dot{\varepsilon}_\theta$ are the axial, radial and hoop strain rates. These values were calculated from the applied stress rates as follows:

$$\dot{\varepsilon}_\text{z} = S_{\text{rz}}\dot{\sigma}_\theta + S_{\text{zz}}\dot{\sigma}_\text{z} \quad (2)$$

$$\dot{\varepsilon}_\theta = S_{\text{rr}}\dot{\sigma}_\theta + S_{\text{rz}}\dot{\sigma}_\text{z} \quad (3)$$

$$\dot{\varepsilon}_\text{r} = S_{\text{r}\theta}\dot{\sigma}_\theta + S_{\text{rz}}\dot{\sigma}_\text{z} \quad (4)$$

where $\dot{\sigma}_\text{z}$ and $\dot{\sigma}_\theta$ are the stress rates in the axial and hoop directions and S_{ij} are the material compliance values (see Appendix).

This method was chosen since the primary purpose of the research was to investigate the yield and failure behavior in multi-axial stress states, and direct measures of the strains was not possible without equipment damage. Consequently, consistent with uniaxial testing where crosshead speed of the test frame is set and maintained constant, similar rates were set and maintained constant in this study. For this reason, we refer to the strain rate as the nominal strain rate. It is acknowledged that this introduces some uncertainty into the actual rates during yielding, but it is also noted that it requires roughly an order of magnitude change in the rate in order to alter the measurable yield stress by approximately 10%.

3. Results and discussion

3.1. Testing at 20°C, 0.05 min^{-1}

Samples were tested at room temperature (20°C) at an octahedral shear strain rate of 0.05 min^{-1}. Fig. 3a plots the octahedral shear yield stress as a function of the mean stress. The octahedral shear stress, τ^{oct}, and mean stress, σ_m, can be written as follows:

$$\tau^{\text{oct}} = \frac{1}{3}\sqrt{(\sigma_\text{z} - \sigma_\theta)^2 + (\sigma_\text{z})^2 + (\sigma_\theta)^2} \quad (5)$$

$$\sigma_\text{m} = \frac{1}{3}(\sigma_\text{z} + \sigma_\theta) \quad (6)$$

where σ_z and σ_θ are the principal stresses in the axial and hoop directions (see Appendix). In studying

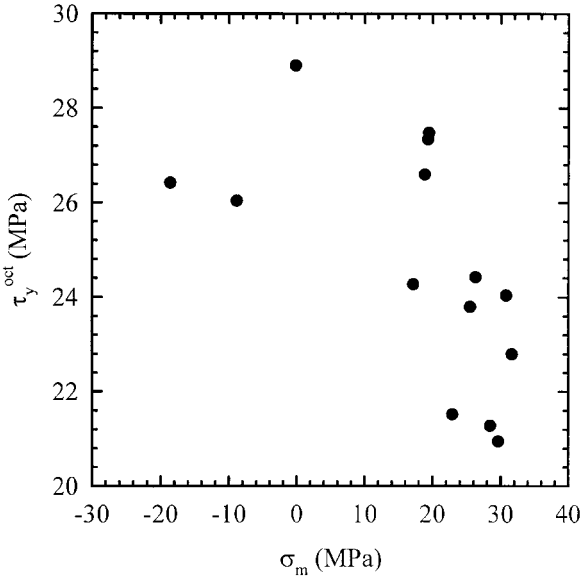

(a)

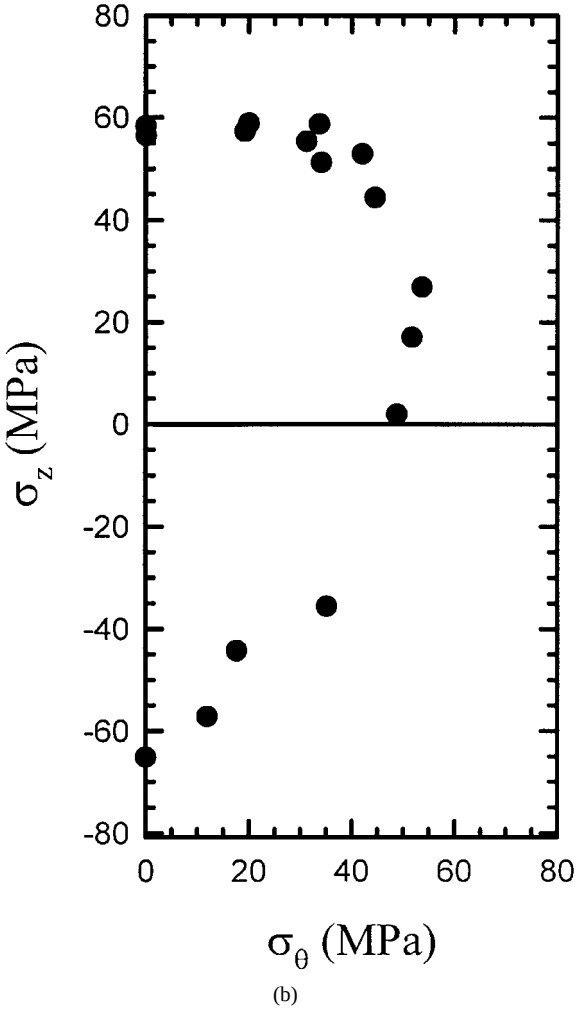

(b)

Figure 3 (a) Octahedral shear stress at yield versus hydrostatic pressure at yield for Carilon hollow cylinders tested at 20°C and $\dot{\gamma}^{oct} = 0.05\ min^{-1}$; (b) Axial stress at yield versus hoop stress at yield for Carilon hollow cylinders tested at 20°C and $\dot{\gamma}^{oct} = 0.05\ min^{-1}$.

the yield behavior of various polymers, other investigators [3, 4] have found a linear relationship between τ_y^{oct} and σ_m. Such a linear dependence, with the slope referred to as the coefficient of internal friction, indicates a modified von Mises type of behavior. Our data do not show this type of relationship, however. While τ_y^{oct} appears to be dependent upon the pressure, a linear dependence is not clear. Rather, the relationship between yield stress and pressure appears to be convoluted due to processing effects which have introduced significant anisotropy in both the stiffness and yield behavior. Others [2, 13] have previously suggested that a linear relationship as described above does not exist in the case of anisotropic polymers. For such reasons, a more suitable way to present the data is in the form of hoop yield stress versus axial yield stress (Fig. 3b).

The observed mode of failure was shown to be closely related to the stress state under which the cylinders were tested. Under uniaxial compression and tension (axial and hoop) as well as equibiaxial tension, ductile yield was observed in the stress-strain response and significant inelastic deformation was observed after the tests were terminated. However, other stress states revealed a more "brittle-type" response. Fig. 4 illustrates cylinder failures for a range of stress states. The dashed lines indicate the loading path under which the specimens were tested. Notice that testing in region I produced failures which appear ductile, while testing under stress states in region II resulted in brittle behavior. For example, necking was observed in the case of axial tension. Significant drawing was also observed for uniaxial tension in the hoop direction. The specimen shown in Fig. 4 which had been tested in region II was loaded under the condition $\sigma_z/\sigma_\theta = 2$ and indicates a brittle failure. Such

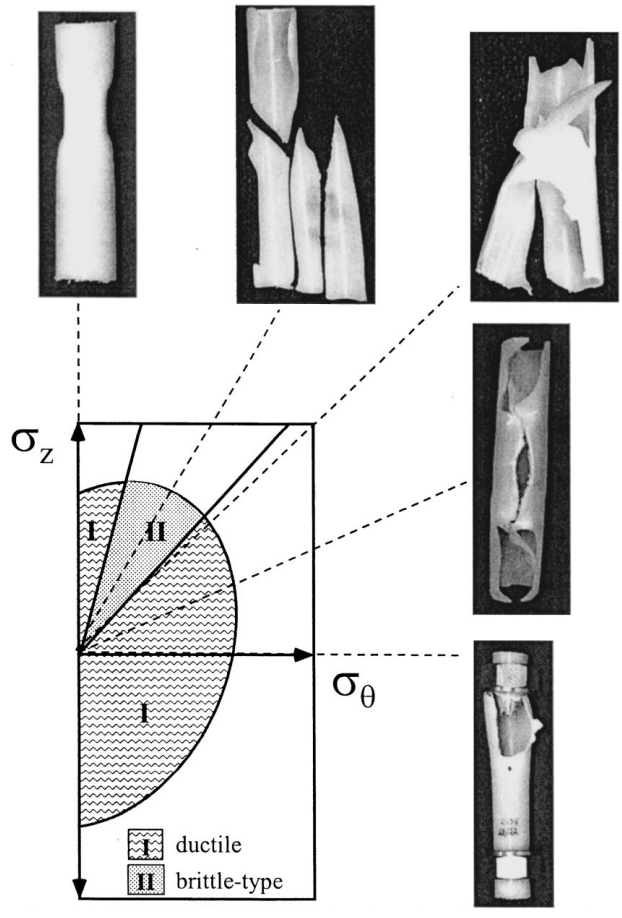

Figure 4 Specimens tested in various stress states at 20°C and $\dot{\gamma}^{oct} = 0.05\ min^{-1}$. Region I indicates the ductile regime, region II indicates the brittle-like regime, and dashed lines represent the loading paths for the corresponding cylinders.

brittle failures showed little evidence of irreversible deformation. Similar results were obtained by others [2] in a study of polycarbonate cylinders. In this study it was found that all of the specimens tested had failed in a ductile manner except one which had been tested within the region we have labeled as region II. The brittle behavior was attributed to excessive aging during thermal treatment, but no explanation was given as to why the other specimens were not affected in a similar fashion. There was no report of any other samples tested within the range of stress states for which our specimens demonstrated brittle behavior.

Fig. 5a illustrates the volumetric strain, ε_v, versus octahedral shear stress, τ^{oct}, response for Carilon tested in various stress states applied at the same octahedral shear strain rate of 0.05 min^{-1} at 20°C. The volumetric strain may be calculated as the sum of the principal strains in the axial, hoop and radial directions, (see Appendix):

$$\varepsilon_v = \varepsilon'_z + \varepsilon'_\theta + \varepsilon'_r \tag{7}$$

As expected, at higher positive values of ε_v, the yield stress value is reduced. It is also evident from this figure that ductile yield behavior as determined by a zero slope condition in the curve was not always realized. Curves that do not display a slope of zero are indicated by dashed lines, and the failures are considered brittle-type. However, the brittle-type response does not correspond to the highest level of volumetric strain. It is typically observed that the more constrained

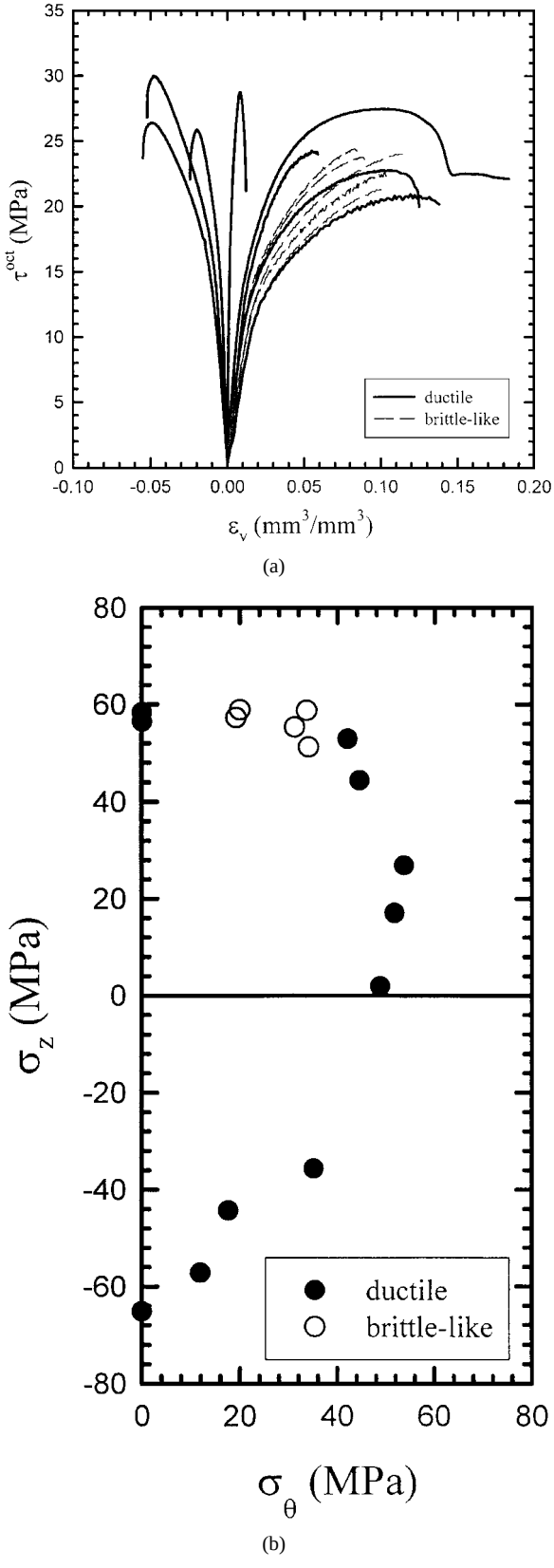

Figure 5 (a) Octahedral shear stress as a function of volumetric strain for hollow cylinder specimens tested at 20°C and octahedral shear strain rate of 0.05 min^{-1}; (b) Axial stress at yield versus hoop stress at yield for Carilon hollow cylinders tested at 20°C and $\dot{\gamma}^{oct} = 0.05$ min^{-1}. Solid symbols represent ductile yield and hollow symbols represent brittle-like failure.

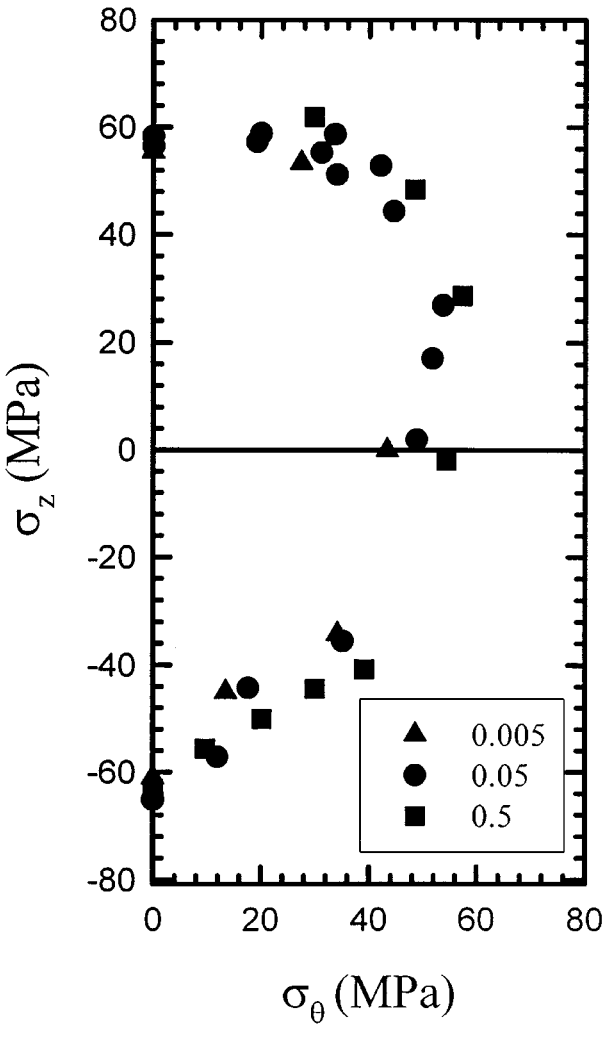

Figure 6 Axial stress at yield versus hoop stress at yield for octahedral shear strain rates of 0.005, 0.05 and 0.5 min^{-1} at 20°C.

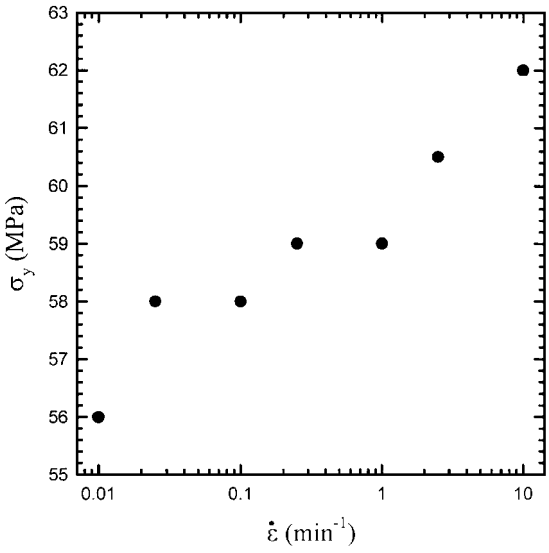

Figure 7 Yield stress as a function of axial strain rate for Carilon tensile bars.

stress states (i.e., those with the highest dilatational component) are most likely to promote brittle type failures, while yielding is associated with a deviatoric material response. The fact that our observations do not follow this trend is believed to be associated with either the anisotropic character of the material or by imposed residual stresses. Fig. 5b plots the axial and hoop stress data, differentiating between ductile and brittle behavior, which correspond to the regions shown in Fig. 4.

3.2. Effect of strain rate

The yield stresses in the axial and hoop directions for the cylinders tested at $\dot{\gamma}^{oct} = 0.005, 0.05,$ and $0.5\,\text{min}^{-1}$ at 20°C are plotted in Fig. 6. An increase in yield strength with strain rate is evident, as expected. However, this difference is not very large considering that the rates vary over 2 orders of magnitude. Small increases in yield strength with increased strain rate were

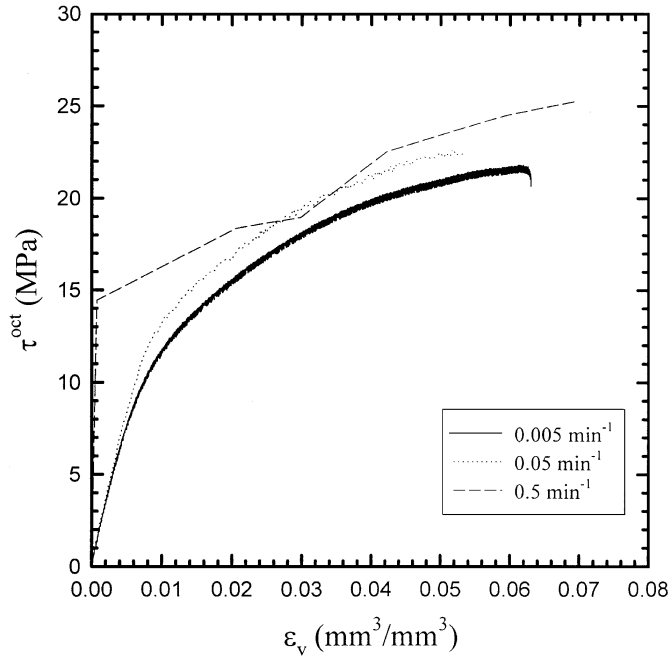

(a)

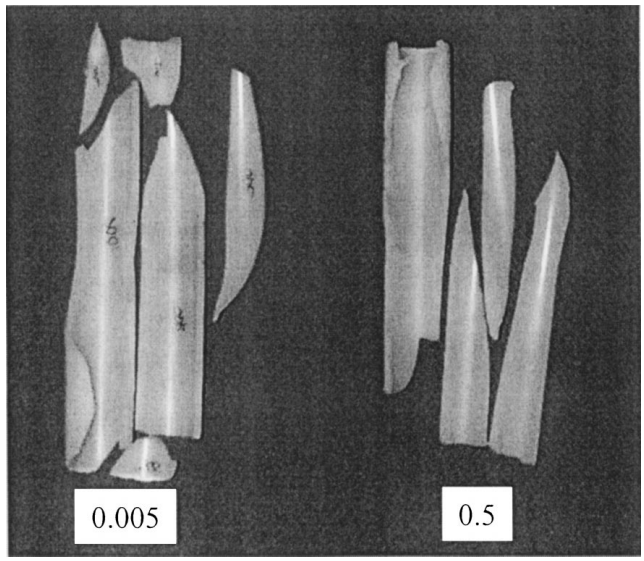

(b)

Figure 8 (a) Octahedral shear stress as a function of volumetric strain for specimens tested at 20°C at octahedral shear strain rates of 0.005, 0.05, and 0.5 min^{-1} for the case of $\sigma_z/\sigma_\theta = 2$; (b) Specimens tested at 20°C at octahedral shear strain rates of 0.005 and 0.5 min^{-1} for the case of $\sigma_z/\sigma_\theta = 2$.

also observed in tensile bar specimens tested over a wider range of rates (Fig. 7). Again, while the strain rate varies over several orders of magnitude, σ_y increases by only a few MPa. Additionally, the cylinders' sensitivity to strain rate effects on the yield stress appears to be greater in the hoop direction than the axial direction. Again, this difference in yielding in the axial and hoop directions is attributed to the anisotropy introduced during extrusion of the test specimens.

At all rates the observed failures for hollow cylinders were predominantly ductile. However, brittle behavior was consistently observed for the case of $\sigma_z/\sigma_\theta = 2$. Fig. 8a and b illustrate the stress-strain curves and the observed failures for specimens subjected to this stress state at different strain rates.

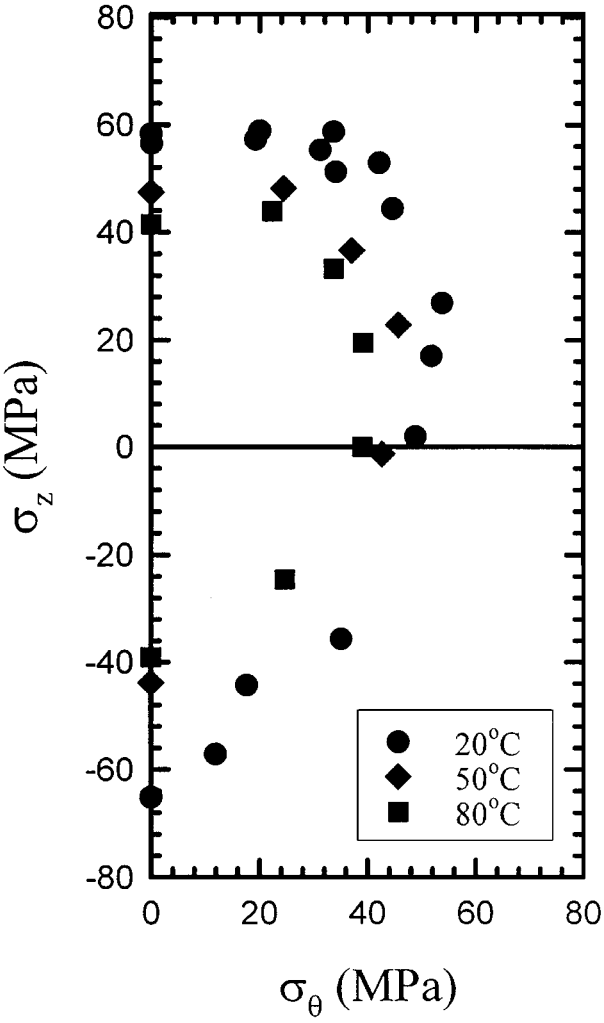

Figure 9 Axial stress at yield versus hoop stress at yield for hollow cylinders tested at temperatures of 20, 50 and 80°C.

3.3. Effect of temperature

The test temperature affected the yield strength of the polymer more significantly than the strain rate. The hoop and axial stresses at yield for specimens tested at 20, 50 and 80°C are plotted in Fig. 9. It is interesting to note that the effect of strain rate was more pronounced in the hoop direction, while the effect of temperature was much greater in the axial direction. We believe this is due to the anisotropic character of the material and, in particular, the morphology of the amorphous phase. The amorphous orientation induced during the extrusion process essentially alters the internal energy of the material through entropic considerations. Thus one should expect that testing the material at different temperatures would not produce similar results as testing the material at different rates in this case.

Specimens tested at 50 and 80°C were found to behave in a ductile manner for all stress states studied. Interestingly, neck formation was observed in the stress state ($\sigma_z/\sigma_\theta = 2$) which previously resulted in brittle behavior at all rates at room temperature. The necks produced at this stress state are of larger diameter than the necks produced in axial tension as a result of the constraint on the material due to internal pressurization (Fig. 10).

At 0°C, failure was typically brittle, with specimens fracturing into many small pieces. As this is below the polymer glass transition temperature of approximately 12°C, brittle behavior was expected. A small amount of irreversible deformation was evident in the case of hoop tension, however. The hoop and axial stresses at yield for specimens tested at 0, 20, 50 and 80°C are plotted in Fig. 11.

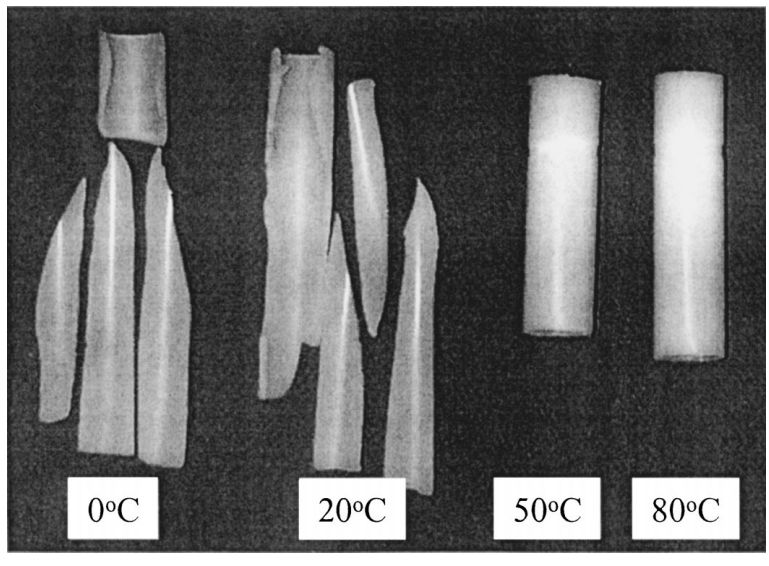

Figure 10 Specimens loaded along $\sigma_z/\sigma_\theta = 2$ at temperatures of 0, 20, 50 and 80°C.

TABLE I Uniaxial tensile data from various testing procedures. Specimen geometry differs between each of the studies

	Carilon tensile bar		Carilon hollow cylinder		Kalay and Bevis 15		Danforth *et al.* 14	
T (°C)	σ_y (MPa)	E (GPa)	σ_y (MPa)	E (GPa)	σ_y (MPa)	E (GPa)	σ_y (MPa)	E (GPa)
0	71	N/A	N/A	2.56	N/A	N/A	64.7	N/A
20 [23]	59	1.4	60.9	1.61	[59.3]	[1.83]	[62]	[1.7]
50	53.5	0.98	47.3	1.06	N/A	N/A	N/A	N/A
80	46.3	0.69	41.4	0.89	47.7	1.1	N/A	N/A

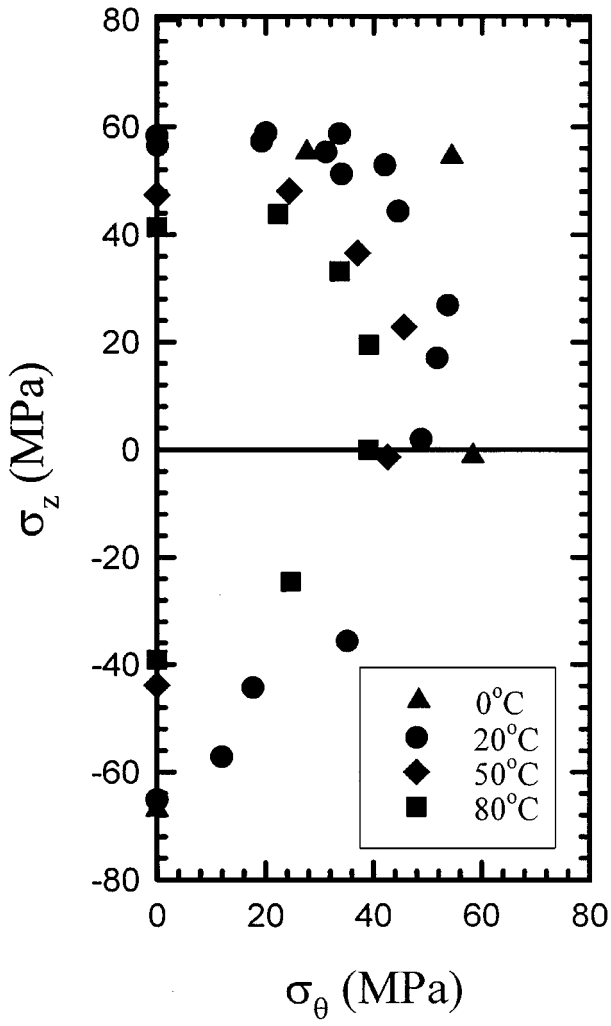

Figure 11 Axial stress at yield versus hoop stress at yield for hollow cylinders tested at temperatures of 0, 20, 50 and 80°C.

The uniaxial tensile data at the various temperatures seem to be in good agreement with the uniaxial tensile data from other studies [14, 15] (Table I). It should be noted, however, that different specimen geometries were used in each of these studies.

Finally, it is not believed that conditioning the samples at higher temperatures has significant effect on the crystallinity of the samples. The temperatures used in this study are significantly below the melting temperature of the material (225°C). It is known that this material undergoes a crystal transformation at approximately 110°C [16], however, differential scanning calorimetry work has not shown any significant features in the temperature range studied here. Additionally, the crystallization of this material is known to be very rapid [17]. It not expected that much difference in crystallinity would arise from different processing or preparation conditions.

4. Conclusions

The purpose of this study was to evaluate the yield behavior of an anisotropic polymeric material subjected to multiaxial stress states. The effects of temperature and test rate on the material response have been investigated. Changes in $\dot{\gamma}^{oct}$ affected τ_y^{oct}, but did not seem to affect the mode of failure. Specimens loaded in the same stress states but at varying rates behaved similarly. However, the temperature had significant effect on both τ_y^{oct} and the mode of failure. Additionally, the effect of strain rate on the yield stress was more pronounced in the hoop direction, whereas the effect of temperature was greater in the axial direction.

Acknowledgements

The authors wish to acknowledge Shell Chemical Company for support of this study. We would also like to thank Piero Puccini and C. C. (James) Kau of Shell Chemical Company for informative discussions.

Appendix

For a thin walled hollow cylinder, combined axial loading and internal pressurization results in the following stresses in the axial and hoop directions:

$$\sigma_z = \frac{Q}{\pi Dt} + \frac{pD}{4t} \tag{A1}$$

$$\sigma_\theta = \frac{pD}{2t} \tag{A2}$$

where Q is the applied axial load, p is the internal pressure, D is the mean diameter, and t is the cylinder thickness. Radial stresses are considered negligible. In the absence of applied torsion, σ_z and σ_θ are the principal stresses. The octahedral shear stress, τ^{oct}, and hydrostatic stress, σ_m, can therefore be written as follows:

$$\tau^{oct} = \frac{1}{3}\sqrt{(\sigma_z - \sigma_\theta)^2 + (\sigma_z)^2 + (\sigma_\theta)^2} \tag{A3}$$

$$\sigma_m = \frac{1}{3}(\sigma_z + \sigma_\theta) \tag{A4}$$

The principal strain values may also be determined. As it is reasonable to expect an extruded pipe to display transverse isotropy, this case will be considered. In cylindrical coordinates, Hooke's law for a transversely

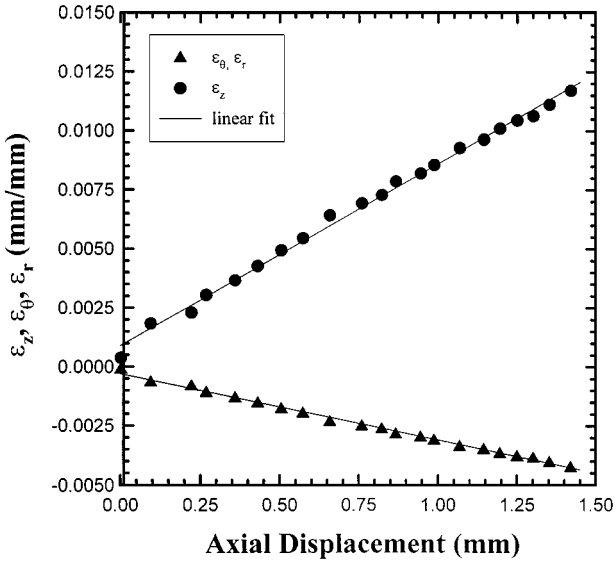

Figure 12 Linear region of plot of principal strain (Equations A9–A11) as a function of axial displacement. The slopes are used in the final calculation of the strain (Equations A12–A14).

isotropic material, neglecting shear terms, may be written as:

$$\begin{Bmatrix} \sigma_r \\ \sigma_\theta \\ \sigma_z \end{Bmatrix} = \begin{bmatrix} C_{rr} & C_{r\theta} & C_{rz} \\ C_{r\theta} & C_{rr} & C_{rz} \\ C_{rz} & C_{rz} & C_{zz} \end{bmatrix} \begin{Bmatrix} \varepsilon_r \\ \varepsilon_\theta \\ \varepsilon_z \end{Bmatrix} \quad \text{(A5)}$$

where C_{rr}, $C_{r\theta}$, C_{rz}, and C_{zz} are 4 of the 5 independent material coefficients, and ε_z, ε_θ and ε_r are the strains in the axial, hoop and radial directions, respectively. Note that for a transversely isotropic material the remaining independent coefficient relates the shear stresses to the strains. In this study samples have been loaded only in the principal directions, hence this coefficient has not been employed. Shear components are thus not within the scope of the present work.

In uniaxial tension, σ_z is the only applied stress. Thus, the following equations are obtained from Hooke's law:

$$\sigma_z = C_{rz}\varepsilon_r + C_{rz}\varepsilon_\theta + C_{zz}\varepsilon_z \quad \text{(A6)}$$

$$\sigma_r = 0 = C_{rr}\varepsilon_r + C_{r\theta}\varepsilon_\theta + C_{rz}\varepsilon_z \quad \text{(A7)}$$

$$\sigma_\theta = 0 = C_{r\theta}\varepsilon_r + C_{rr}\varepsilon_\theta + C_{rz}\varepsilon_z \quad \text{(A8)}$$

Similar equations may also be written for other states of stress. With these equations, the stiffness matrix, **C**, can be determined. Inversion of the matrix yields the compliance matrix, **S**, from which the principal strains may be calculated using Hooke's law:

$$\varepsilon_z = S_{rz}\sigma_\theta + S_{zz}\sigma_z \quad \text{(A9)}$$

$$\varepsilon_\theta = S_{rr}\sigma_\theta + S_{rz}\sigma_z \quad \text{(A10)}$$

$$\varepsilon_r = S_{r\theta}\sigma_\theta + S_{rz}\sigma_z \quad \text{(A11)}$$

where S_{ij} are components of the compliance matrix. These equations are for the case of a transversely isotropic material in the absence of shear. Again, radial stresses are considered negligible. However, these equations are valid only in the linear elastic regime, and the testing performed in this study extends into the non-linear region. To account for this non-linearity, the strains were assumed to scale with the displacement, δ, with scale factors obtained from the linear portion of plots of the strains calculated using Equations (A9–A11) vs. crosshead displacement (Fig. 12 is an example of such a plot for the case of uniaxial tension). Therefore, the experimental principal strain values are calculated as:

$$\varepsilon_z' = m_z\delta \quad \text{(A12)}$$

$$\varepsilon_\theta' = m_\theta\delta \quad \text{(A13)}$$

$$\varepsilon_r' = m_r\delta \quad \text{(A14)}$$

where m_z, m_θ and m_r are the slopes of the plot of ε_z, ε_θ and ε_r (respectively) vs. δ. Strain values calculated in this manner compared well with those measured with extensometers for the case of axial tension in tensile bars.

References

1. P. B. BOWDEN and J. A. JUKES, *J. Mater. Sci.* **3** (1968) 183.
2. L. M. CARAPELLUCCI and A. F. YEE, *Polym. Eng. Sci.* **26** (1986) 920.
3. R. S. KODY and A. J. LESSER, *J. Mater. Sci.* **32** (1997) 5637.
4. A. J. LESSER and R. S. KODY, *J. Polym. Sci.: Part B: Polym. Phys.* **35** (1997) 1611.
5. R. K. MITTAL and I. P. SINGH, *Polym. Eng. Sci.* **22** (1982) 358.
6. M. E. TUTTLE, M. SEMELISS and R. WONG, *Exp. Mechan.* **March** (1992) 1.
7. N. E. BEKHET, D. C. BARTON and G. CRAGGS, *J. Mater. Sci.* **29** (1994) 4953.
8. C. ASH, *Intern. J. Polym. Mater.* **30** (1995) 1.
9. C. E. ASH and J. E. FLOOD, *Polym. Matls. Sci. and Eng.* **76** (1997) 110.
10. F. GARBASSI and A. SOMMAZZI, *Polym. News* **20** (1994) 201.
11. J. W. KELLEY, D. R. ROANE and D. M. LE, in 53rd ANTEC, 1995, p. 3819.
12. R. RAGHAVA, R. M. CADDELL and G. S. Y. YEH, *J. Mater. Sci.* **8** (1973) 225.
13. R. M. CADDELL, R. S. RAGHAVA and A. G. ATKINS, *ibid.* **8** (1973) 1641.
14. R. L. DANFORTH, J. M. MACHADO and J. C. M. JORDAAN, *Plast. Eng.* **March** (1996) 77.
15. G. KALAY and M. BEVIS, *J. Polym. Sci.: Part B: Polym. Phys.* **35** (1997) 415.
16. E. A. KLOP, B. J. LOMMERTS, J. VEURINK, J. AERTS and R. R. VAN PUIJENBROEK, *ibid.* **33** (1995) 315.
17. G. A. HOLT and J. E. SPRUIELL, *Polym. Matls. Sci. and Eng.* **76** (1997) 112.

Received 23 February
and accepted 2 November 1999